Regional Hypoxia in Glioblastoma Multiforme Quantified with [^{18}F]Fluoromisonidazole Positron Emission Tomography before Radiotherapy: Correlation with Time to Progression and Survival

Alexander M. Spence,[1] Mark Muzi,[2] Kristin R. Swanson,[3] Finbarr O'Sullivan,[6] Jason K. Rockhill,[4] Joseph G. Rajendran,[2] Tom C.H. Adamsen,[2] Jeanne M. Link,[2] Paul E. Swanson,[3] Kevin J. Yagle,[2] Robert C. Rostomily,[5] Daniel L. Silbergeld,[5] and Kenneth A. Krohn[2]

Abstract

Purpose: Hypoxia is associated with resistance to radiotherapy and chemotherapy and activates transcription factors that support cell survival and migration. We measured the volume of hypoxic tumor and the maximum level of hypoxia in glioblastoma multiforme before radiotherapy with [^{18}F]fluoromisonidazole positron emission tomography to assess their impact on time to progression (TTP) or survival.

Experimental Design: Twenty-two patients were studied before biopsy or between resection and starting radiotherapy. Each had a 20-minute emission scan 2 hours after i.v. injection of 7 mCi of [^{18}F]fluoromisonidazole. Venous blood samples taken during imaging were used to create tissue to blood concentration (T/B) ratios. The volume of tumor with T/B values above 1.2 defined the hypoxic volume (HV). Maximum T/B values (T/B_{max}) were determined from the pixel with the highest uptake.

Results: Kaplan-Meier plots showed shorter TTP and survival in patients whose tumors contained HVs or tumor T/B_{max} ratios greater than the median ($P \leq 0.001$). In univariate analyses, greater HV or tumor T/B_{max} were associated with shorter TTP or survival ($P < 0.002$). Multivariate analyses for survival and TTP against the covariates HV (or T/B_{max}), magnetic resonance imaging (MRI) T1Gd volume, age, and Karnovsky performance score reached significance only for HV (or T/B_{max}; $P < 0.03$).

Conclusions: The volume and intensity of hypoxia in glioblastoma multiforme before radiotherapy are strongly associated with poorer TTP and survival. This type of imaging could be integrated into new treatment strategies to target hypoxia more aggressively in glioblastoma multiforme and could be applied to assess the treatment outcomes.

Hypoxic tumor cells are resistant to ionizing radiation and chemotherapy relative to well-oxygenated cells (1–3). For several human cancers, it has been shown that low oxygen tension is associated with persistent tumor following radiotherapy and the subsequent development of local recurrences and metastases (4–6). Spontaneous necrosis in glioblastoma multiforme is a frequent finding and is thought to result from diffusion-limited hypoxia (7). Solid proof that glioblastomas contain hypoxic regions came from Rampling et al. (8) who used polarographic electrodes to show that 9.5% to 68.5% (median 39.5%) of pO_2 measurements at multiple sites in tumors from 10 patients yielded values <2.5 mm Hg.

Evans et al. (9) reported similar results from electrode measurements but could not establish a relationship between hypoxia measured with needle electrodes and tumor grade. Needle electrode studies are invasive and limited to accessible tumor sites. They provide limited regional information and only indirectly suggest a relationship to tumor grade and survival. Also, needle electrode studies are not easily repeatable or amenable to routine clinical application.

The discovery in the mid 1980s that some radiosensitizing drugs (e.g., misonidazole) are selectively bound to molecules in viable hypoxic cells *in vitro* and *in vivo* attracted interest not only from radiation biologists but also from the nuclear medicine specialists (10, 11). Early studies showed that fluoromisonidazole binds stably in the same populations of hypoxic cells as misonidazole, leading to the conclusion that [^{18}F]fluoromisonidazole (FMISO) is useful as a noninvasive hypoxia imaging agent with positron emission tomography (PET; ref. 11). Its binding is proportional to the level of hypoxia and substantial retention occurs at oxygen levels of 3 mm Hg and below (12), although some estimates suggest binding at levels as high as 10 mm Hg (13). This is the same pO_2 range over which the oxygen enhancement ratio of

Authors' Affiliations: Departments of [1]Neurology, [2]Radiology, [3]Pathology, [4]Radiation Oncology, and [5]Neurosurgery, University of Washington, Seattle, Washington; and [6]Department of Statistics, University College Cork, Cork, Ireland
Received 12/4/07; revised 1/15/08; accepted 1/17/08.

Grant support: NIH grants P01 CA42045 and S10 RR17229.

The costs of publication of this article were defrayed in part by the payment of page charges. This article must therefore be hereby marked *advertisement* in accordance with 18 U.S.C. Section 1734 solely to indicate this fact.

Requests for reprints: Alexander M. Spence, Department of Neurology, 356465, University of Washington, Seattle, WA 98195. Phone: 206-543-2340; Fax: 206-685-8100; E-mail: aspence@u.washington.edu.

doi:10.1158/1078-0432.CCR-07-4995

radiation changes from 3 (above 10 mm Hg) to 1 (below 1 mm Hg; ref. 14).

Hypoxia at these levels is sufficient to cause significant radioresistance and to increase activity of the important transcription factor, hypoxia-inducible factor-1 (HIF1). The HIF1α subunit survives ubiquitination as oxygen concentration decreases, leading to heterodimerization with HIF1β to form HIF1, which binds to hypoxia response elements of ~100 genes whose protein products increase oxygen availability or help adapt to insufficient levels of oxygen (15). These include genes for vascular endothelial growth factor (VEGF), glycolytic enzymes, glucose transporters, carbonic anhydrase 9, erythropoietin, insulin like growth factor II, and insulin-like growth factor binding proteins (15–17). Thus, hypoxia via multiple downstream effects imposes a significant barrier to successful therapy for many cancers, including glioblastoma multiforme.

The hypothesis for this report is that the burden of hypoxic tissue in glioblastoma multiforme quantified regionally with FMISO PET as either hypoxic volume (HV) or maximum tissue to blood concentration ratio (T/B_{max}) is inversely related to time to tumor progression (TTP) and survival. This has long been suspected and is supported by the following results.

Materials and Methods

Patients. This work focuses on 22 patients, all with glioblastoma multiforme, studied with FMISO PET either before or after biopsy alone, or after resection before treatment with radiotherapy. The imaged tumors therefore represent all the disease present at the time preceding radiotherapy (i.e., that left following surgery). There were 13 males and 9 females, age range 41 to 77 years, median 56. Karnovsky performance scores (KPS) ranged from 60 to 100, median 70. The patients were recruited from the University of Washington Medical Center, Harborview Medical Center, and the Veterans' Administration Puget Sound Health Care System. All signed informed consent approved by the Investigational Review Board and Radiation Safety committees.

The majority of patients received 59.4 to 61.2 Gy standard external beam fractionated radiotherapy after the FMISO imaging. One patient died before starting radiotherapy; one received only one fraction of 1.8 Gy; and one received only 30 Gy. Two patients received 15 neutron Gy followed by 14.4 photon Gy radiotherapy (18). Fifteen patients received temozolomide chemotherapy and one received carmustine [1,3-bis(2-chloroethyl)-1-nitrosourea]. Eighteen patients were receiving dexamethasone at the time of the FMISO study. TTP and survival were calculated from the date of diagnostic surgery. Progression was defined by MRI criteria (19).

PET imaging. Patients were imaged in the supine position with head immobilization achieved by using a moldable thermoplastic mask. All PET scans were done on an Advance tomograph (G.E. Medical Systems) operating in three-dimensional, high-resolution mode with 35 imaging planes covering a 15-cm axial field of view. Performance characteristics of the tomograph have been published elsewhere (20). Attenuation scans with a Ge-68 rotating sector source were also obtained. All emission images were reconstructed with a Hanning filter after corrections for scatter, singles, and random events, resulting in a reconstructed spatial resolution of ~6 mm (20). The tomograph is regularly calibrated to convert cpm/pixel to μCi/mL using large vials containing known activities of ^{18}F imaged separately from the patient and reconstructed using the same filter as the emission images.

FMISO protocol. [^{18}F]FMISO was prepared by a modification of the method of Lim and Berridge (21, 22). Venous access lines were placed in each arm, one for FMISO injection and the other for blood sampling. Patients were injected i.v. with 3.7 MBq/kg (0.1 mCi/kg) of [^{18}F]FMISO (maximum 260 MBq, 7 mCi). A single field-of-view emission scan from 120 to 140 min postinjection and an attenuation scan (25 min) of the brain with tumor were obtained. The acquired imaging data were reconstructed to determine the tumor HV as described below. During emission tomography, four venous blood samples were obtained at intervals of 5 min. Whole blood samples of 1 mL each were counted in a Cobra multichannel gamma well counter (Packard Corp.) that is calibrated each week in units of cpm/μCi. Blood activity was averaged and then expressed as μCi/mL decay corrected to time of injection.

Image analysis. MRIs were coregistered with the FMISO images to delineate tumor and brain regions of interest (ROI). These regions of interest were drawn using Alice imaging software (HIPG) over the entire tumor volume. FMISO images and blood activity data were decay corrected to the time of injection and converted to μCi/mL. The FMISO image data were divided by the average blood value to produce tissue/blood (T/B) values. This allowed a pixel-by-pixel calculation of T/B activity ratios for all image planes. The number of pixels in the tumor volume with a T/B ratio $\geq$1.2, indicating significant hypoxia, was determined and converted to milliliter units to measure the HV. Because FMISO has a partition coefficient of 0.41 in normal oxygenated tissues, the concentrations in tissue and blood rapidly equilibrate and are essentially identical a short time after injection (23). The cutoff ratio of 1.2 was based on T/B ratios previously measured with the G.E. Advance tomograph in normal brain and muscle where >90% of the values fell below 1.1 (24). This very simple analysis is one of the strengths of the FMISO study. In each tumor region, we also located the pixel with the maximum T/B ratio and included this variable, T/B_{max}, in our analysis. HV depicts the volume of tumor that has crossed the threshold for hypoxia and T/B_{max} depicts the magnitude of the hypoxia.

MRI images in 17 patients whose scans were within 2 wk of the FMISO images were processed for measuring the volumes of T0, T1Gd, and T2 by standard methods.[7] T0 represents the hypointense necrotic volume on T1 images; T1Gd includes all the contrast enhancing volume associated with blood-brain barrier disruption excluding the necrotic volume; and T2 is all the tumor within the bounds of T2 including the T0 and T1Gd volumes. T2-T0 therefore amounts to all of the nonnecrotic tumor detected by MRI.

Immunocytochemistry analysis. From the first 19 patients of this report, paraffin sections of the tumor specimens were processed for immunocytochemistry for the following: VEGF, HIF1α, Ki67 antigen, and p53. These were sectioned, deparaffinized, rehydrated, and then treated in 3% hydrogen peroxide to block endogenous peroxidase activity. Slides were subjected to antigen retrieval by heating in Target Retrieval Solution (pH 6; DAKOCytomation), followed by a rinse with dH_2O and then TBS. The primary antibody was diluted appropriately (1:500 for VEGF, 1:1,000 for HIF1α in blocking buffer; DAKO Corp.) and incubated overnight at 4°C. Following several TBS washes, slides were loaded to a DAKO Autostainer and detected with CSA II reagents (DAKO-Cytomation) according to manufacturer's specifications (horseradish peroxidase–conjugated anti-mouse, amplification reagent, anti–fluorescein-horseradish peroxidase, and finally 3,3′-diaminobenzidine chromogen).

The slides were scored by a trained pathologist using a four-point system for stain intensity: 0, 1, 2, and 3 (for no staining, light, medium, or dark staining). The staining pattern was scored by assigning it to three rather broad categories without numerical value: rare/focal (0-25% tumor cells stained), variable (25-75% stained), and uniform (>75% stained; ref. 25). Additionally, both stain intensity and stain pattern were assigned numerical scores according to the algorithm of Allred and colleagues (26, 27). The overall intensity is scored the same as above, with values from 0 to 3. The scoring for extent of stain is given a numerical value, and is divided into six categories rather than three: no stain, 0; ≤1/100 cells stained, 1; ≤1/10 cells stained, 2; ≤1/3 cells

[7] Swanson et al., in preparation.

Table 1. Patient age, sex, performance status, extent of resection, radiotherapy history, TTP, survival, T/B_{max}, and HV

No.	Age	Sex	KPS	Extent of resection	RT (Gy)	TTP (mo)	Survival (mo)	T/B_{max}	HV (cm^3)
1	49	F	80	GT	15 nGy + 14.4 Gy photon	5	5.4	2.0	6.3
2	47	F	100	GT	15 nGy + 14.4 Gy photon	9.5	13.4	1.2	0.1
3	63	M	90	Bx	59.4	3	3.8	4.2	50.4
4	44	F	80	ST	61.2	7.3	13.4	1.4	2.9
5	72	M	70	Bx		1.4	1.4	3.5	58.0
6	53	M	100	GT	61.2	10	13.6	1.6	5.3
7	55	F	70	Bx	59.4	3	4.4	3.0	129.3
8	65	M	60	ST	61.2	7	9.4	2.1	10.1
9	56	M	90	Bx	60.0	14	31.6*	1.6	12.8
10	73	M	60	Bx	59.4	3	7.3	2.9	46.9
11	54	F	70	GT	61.2	30 †	30*	1.6	4.2
12	49	F	80	ST	61.2	5	15.8	2.0	15.2
13	65	M	60	ST	64.8	4.1	8.7	1.7	2.6
14	41	M	100	ST	61.2	15.4	22.4	2.0	11.2
15	68	M	60	Bx	58.8	2.6	4.6	3.2	70.6
16	53	F	70	Bx	61.2	2.7	12.3	2.1	12.9
17	70	M	70	Bx	61.2	13.9	19*	1.6	3.1
18	54	F	70	ST	52.0	1.9	4.1	2.8	98.2
19	76	M	60	Bx	30.0	1.2	2.5	2.2	32.5
20	75	M	70	ST	16.2	0.8	3.6	2.2	27.0
21	77	M	70	ST	1.8	1.1	1.5	3.0	86.6
22	56	F	90	GT	61.2	10.1 †	10.1*	1.6	10.0

Abbreviations: RT, radiotherapy; GT, gross total; ST, subtotal; Bx, biopsy; nGy, neutron gray.
*Alive and censored.
† Without progression and censored.

stained, 3, ≤2/3 cells stained, 4; and all cells stained, 5. The advantage of using the Allred scoring system is that the scores from the two categories (intensity and extent of positive stain) can be combined into a single value, allowing for correlations with other important criteria such as disease progression.

Statistical analysis. Survival and TTP in months were the outcomes in the analysis. These were calculated from the date of surgery and the most recent follow-up information. Progression was defined by MRI criteria (19). All analyses were completed with standard censoring procedures for survival analysis (28). The chief prognostic variables considered in the analysis were FMISO HV and T/B_{max}; age; KPS; extent of resection; and the MRI volumes, T0, T1Gd, T2, and T2-T0.

For univariate analyses, Cox regression was used to assess the significance of individual variables using log-rank tests. Kaplan-Meier curves were plotted to compare TTP and survival in the patients above versus below the median values for the HV, T/B_{max}, and the MRI volumes.

For multivariate analyses, the relation between survival or TTP and the set of measured prognostic factors was evaluated using the standard Cox proportional hazards regression analysis. This analysis permits an examination of the influence of the PET measures while controlling for the effects of other potential prognostic factors. The continuous variables in the multivariate analysis included HV; T/B_{max}; age; KPS; and MRI T0, T1Gd, T2, and T2-T0. Sex, extent of resection, and immunocytochemistry intensities for VEGF, HIF1α, Ki67, and p53 were entered as categorical variables.

Results

All patients had glioblastoma multiforme by WHO criteria. Twenty-one of 22 patients had necrosis, as shown on the pathology review. The one patient lacking necrosis had only a biopsy. By imaging with MRI T1 plus gadolinium, there was a large conspicuous necrotic center in this patient's tumor. The patient age, sex, KPS, extent of resection, radiotherapy history, TTP, survival, HV, and T/B_{max} are shown in Table 1. At the time of this report, 18 patients had succumbed and 20 had shown tumor progression.

Representative images. Figure 1 shows two patients at the extremes of HVs in this series to illustrate the quality of the FMISO images. MRI T1Gd images are included.

Statistical analysis. Kaplan-Meier plots showed shorter survival and TTP in patients whose tumors contained HVs or tumor T/B_{max} ratios greater than the median (HV 12.8 cm^3, T/B_{max} 2.06; $P < 0.0005$; Fig. 2). Similar plots showed that the T1Gd volume was associated with worse survival ($P = 0.05$) but not TTP ($P = 0.15$). T0 and T2 Kaplan-Meier plots are not shown because these showed no significant association with TTP or survival in this type of analysis.

In univariate Cox model regression analyses, greater HV or tumor T/B_{max} were associated with shorter TTP and survival (all $P < 0.003$; Table 2). Age and T1Gd MRI volume were also significant in the survival analysis, whereas age and KPS but not T1Gd were significant in the TTP analysis. T0, T2, and T2-T0 MRI volumes and the extent of resection did not reach significance in either the survival or TTP calculations.

A multivariate linear regression analysis was carried out to assess the amount of information in the HV or T/B_{max} variables that could be explained by MRI volume measurements. The results are shown in Table 3. T1Gd showed a significant positive correlation with FMISO HV. There was no additional information gained by including any other MR data in this analysis and none of the MR volumes correlated with tumor T/B_{max}.

There are a variety of multivariate models that could be considered for our data. Given the very modest sample size, it is

clearly not reasonable to present all possible subsets. To provide an examination of relative effects, we considered models obtained by retaining terms that reached statistical significance (at the 0.05 level) in either univariate survival or TTP analysis. This lead to consideration of multivariate models with FMISO (HV or T/B_{max}), age, KPS, and T1Gd MRI volume as factors. The results of these multivariate models for HV and T/B_{max} are presented in Table 4. The analysis confirms the importance of FMISO HV and T/B_{max} relative to T1Gd and the known prognostic factors of age and KPS ($P < 0.04$). The failure of T1Gd, age, and KPS to reach significance reinforces the strength of the association between HV and T/B_{max} and patient outcome. The multivariate Cox model indicates that an increase in HV on the order of 7 to 8 cm^3 is associated with a 50% reduction in survival or TTP. An increase in T/B_{max} of 0.25 (or 0.35 for TTP) is associated with a 50% reduction in survival (or TTP). Comparison between HV and T/B_{max} models in terms of the logarithm of the partial likelihood shows no clear advantage for either method of quantifying the FMISO results. Further data would be required to clarify this.

Immunocytochemistry results. Ki-67 immunocytochemistry showed high intensity with a range of 5% to 60% positive (median 35%). In the majority, the pattern was variable from region to region. The p53 uptake was variable in intensity but ranged from 0% (one patient) to 80% with a median of 30%. In two tumors, there was uniform high-intensity staining, but the majority showed a variable pattern from region to region. HIF1α showed a pattern of high intensity in six, intermediate in nine, and low in four cases with a percent uptake range of 1% to 55%, median 28%. The intensity of uptake for VEGF was high in 10 cases, intermediate in 6 cases, low in 2 cases, and zero in 1 case. Three tumors showed a uniform distribution; 10 showed a variable distribution; and 5 showed a rare focal pattern. These biomarker variables showed no statistically significant correlations with HV or T/B_{max}.

Discussion

From studies with experimental tumors, our current understanding of the level of hypoxia necessary to cause detectable retention of FMISO is pO_2 in the range of 2 to 3 mm Hg and below (12). FMISO retention could underestimate the full extent of radiobiologically significant hypoxia because there are effects of hypoxia on radiation response in tissue in the range of pO_2 3 to 10 mm Hg. Also, retention of FMISO is affected by (*a*) the time after injection that the images are acquired and (*b*) losses of tracer and/or metabolites from the blood and tissue of interest; however, these effects are minor when retention is normalized to the blood level. Uptake is not affected by the blood-brain or blood-tumor barriers because the

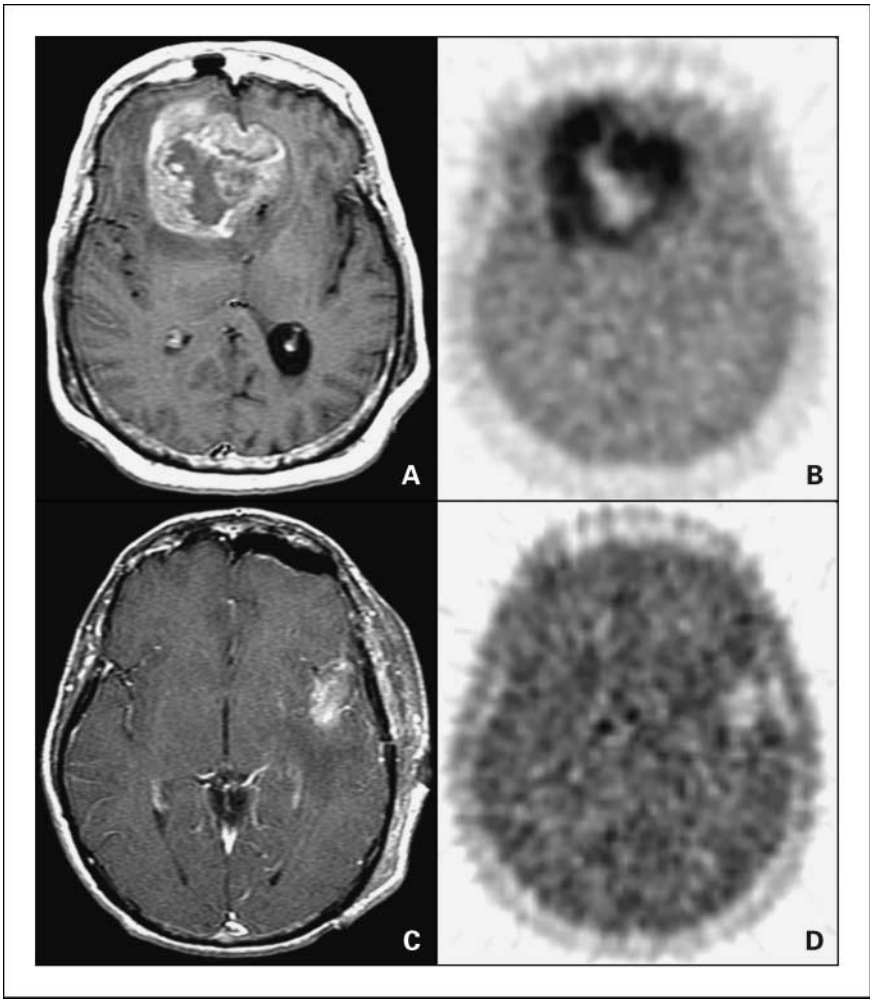

Fig. 1. *A* and *B,* a 55-y-old woman with a bifrontal glioblastoma multiforme imaged after a biopsy. *A,* MRI T1Gd showing a large contrast-enhancing irregular ring-shaped tumor with a necrotic center. The T0 volume was 20 cm^3, T1Gd 80 cm^3, and T2 167 cm^3. *B,* FMISO image through the same plane. The HV was 129 cm^3 and the T/B_{max} was 3.0. *C* and *D,* a 53-y-old man with a left temporal glioblastoma multiforme imaged after a gross total resection. *C,* MRI T1Gd showing only blood products and no residual contrast-positive disease. The T0 volume was 1 cm^3, T1Gd 7 cm^3, and T2 37 cm^3. *D,* FMISO image through the same plane. The HV was 5.3 cm^3 and the T/B_{max} was 1.6.

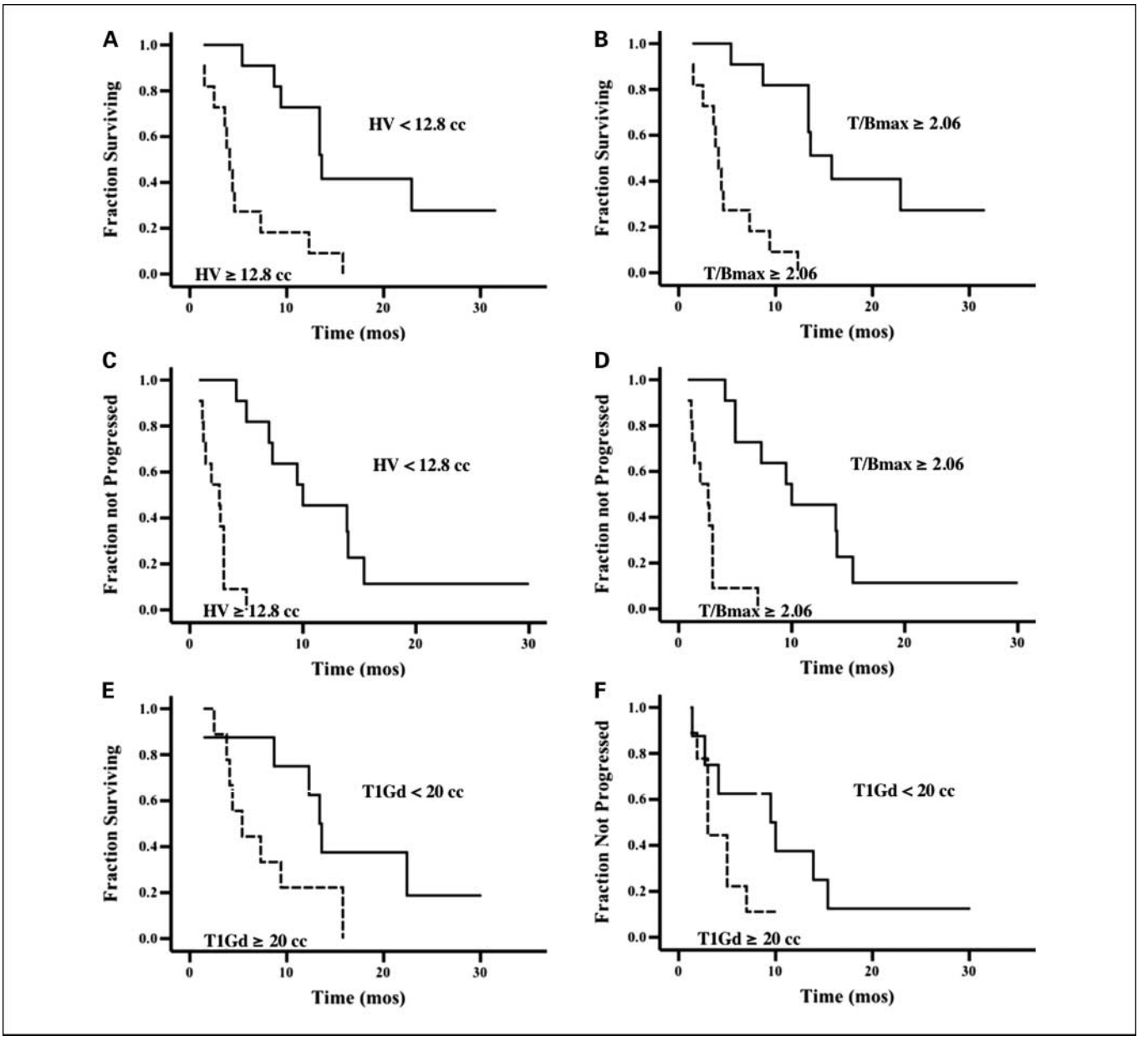

Fig. 2. *A* and *B,* Kaplan-Meier plots of survival versus HV or T/B_{max} show significantly worse survival in patients whose tumors had HV or T/B_{max} values greater than the median ($P < 0.0005$ and 0.0001 respectively; $n = 22$). *C* and *D,* similar plots show that greater HV and T/B_{max} were associated with worse TTP ($P < 0.0001$ for both). *E* and *F,* T1Gd volume was associated with worse survival ($P = 0.05$) but not TTP ($P = 0.15$; $n = 17$).

partition coefficient is 0.41 nor is it affected by perfusion at the 2-hour postinjection time point (29, 30). Based on these considerations and significant experience reported on FMISO from other centers, FMISO retention validly approximates the regional extent and severity of hypoxia in human and animal cancers (24, 29, 31, 32).

This report of 22 patients, all with glioblastoma multiforme, documents that the severity of hypoxic burden measured with FMISO PET after initial surgical intervention significantly impacts time to tumor progression and overall survival. As Table 2 shows, assessments of HV or T/B_{max} individually against survival or TTP in the univariate Cox model all reached significance at $P < 0.003$ or lower. Age and T1Gd of the MRI variables were significant in relation to survival, whereas age and KPS but not the MRI variables were significant in relation to TTP. Multivariate analysis showed HV and T/B_{max} to be important variables strongly associated with survival and TTP compared with the other potential variables, including age, KPS, and the T1Gd MRI volume (Table 4). Together, these results argue that FMISO PET measurements of hypoxia in glioblastoma multiforme before radiotherapy quantify a very important outcome variable and extend our understanding of an important pathophysiologic process beyond what is shown by conventional anatomic imaging.

The multiple regression results (Table 3) show a significant correlation between HV and the MRI T1Gd volume; there is a component of HV information that is associated with tumor burden defined by MRI. However, this result with T1Gd does

Table 2. Univariate Cox model regression analyses of survival or TTP versus HV, T/B_{max}, T0, T1Gd, T2, T2-T0, age, KPS, or extent of resection

	Log hazard ratio coefficient (SE)	P
Survival		
HV	0.024 (0.01)	0.001
T/B_{max}	1.46 (0.400)	0.0002
T0	0.042 (0.064)	0.51
T1Gd	0.03 (0.02)	0.04
T2	0.007 (0.01)	0.44
T2-T0	0.008 (0.01)	0.45
Age	0.056 (0.03)	0.03
KPS	-0.03 (0.02)	0.09
Extent of resection		
GT vs Bx	-0.76 (0.69)	0.27
ST vs Bx	0.07 (0.52)	0.90
TTP		
HV	0.018 (0.01)	0.003
T/B_{max}	0.938 (0.31)	0.003
T0	0.026 (0.06)	0.66
T1Gd	0.022 (0.01)	0.11
T2	0.005 (0.01)	0.53
T2-T0	0.006 (0.01)	0.52
Age	0.065 (0.03)	0.01
KPS	-0.035 (0.02)	0.05
Extent of resection		
GT vs Bx	-1.31 (0.68)	0.06
ST vs Bx	-0.19 (0.51)	0.71

not contradict the above paragraph and is expected because there is a biological link between hypoxia and blood-brain barrier breakdown, both quantitatively and spatially. Simply put, tumor growth leads to cells being pushed beyond the diffusion distance of O_2, which up-regulates the production of cytokines such as VEGF leading to endothelial proliferation and leakage of the blood-brain barrier about which T1Gd shows the regional distribution. A more complete interpretation of the spatial relationships among the MRI volumes and hypoxia variables will require additional studies of their regional heterogeneity.[7]

Prior reports on FMISO PET imaging of gliomas included only small numbers with glioblastoma (29, 31, 33, 34). In the reports of Cher et al. and Bruehlmeier et al., there were seven each, all of which showed uptake of FMISO consistent with our findings (29, 31).

Also, our data are concordant with a series of investigations from the University of Pennsylvania (9, 35, 36). Evans et al. (36) investigated the relationship between extent and severity of hypoxia in 18 untreated gliomas, and time to recurrence as a measure of clinical aggressiveness. Hypoxia was assessed by the binding of the nonradioactive nitroimidazole, EF5 [2-(2-nitro-1-*H*-imidazol-1-yl)-*N*-(2,2,3,3,3-pentafluoropropyl) acetamide], in tumor samples collected after patients had been injected preoperatively with the EF5. Eppendorf needle electrode measurements were also collected intraoperatively. Five of 12 glioblastomas showed severe hypoxia (~0.1% oxygen, 0.8 mm Hg). EF5 binding was always found where necrosis could be identified histopathologically but there was also binding in some areas where necrosis could not be identified. More rapid recurrence was associated with hypoxia, as shown by EF5 binding but not by the measurements with the needle electrodes.

In our survey of the pathology specimens with immunocytochemistry for VEGF, HIF1α, Ki67, and p53, we were unable to prove any correlations with the FMISO HV or T/B_{max} imaging results, or TTP and survival. Based on prior reports, we hypothesized that there would be a relationship between Ki67, HIF1α, and VEGF intensity and distribution and FMISO HV and T/B_{max} (31, 37, 38). VEGF and receptor expression have been shown to correlate with tumor grade in astrocytic gliomas, oligodendroglioma, and ependymoma (17, 39, 40). VEGF expression was seen around necrotic foci and correlated highly with microvessel density and endothelial proliferation. Anaplastic progression was associated with regional expression of VEGF. However, there may well be variations among and within gliomas in the VEGF response to hypoxia (41, 42).

With respect to HIF1α, Zagzag et al. (43) showed in glioblastoma multiforme that it localizes in pseudopalisading cells around areas of necrosis and in tumor cells infiltrating the brain at the tumor margin. Other investigators have confirmed up-regulation of HIF1α mRNA in glioblastoma multiforme compared with lower grade lesions and increased nuclear expression of HIF1α protein especially surrounding necrotic areas (44). The failure of our survey of the immunocytochemical variables to show significant correlations with HV or T/B_{max} could be the result of the small sample size (n = 19) or the specimens being collected without attention to location in relation to the FMISO distribution. Further studies will be necessary to clarify whether there are associations between FMISO uptake and intensity of expression of HIF1α and VEGF, and how strong they are (45).

With robust evidence that the burden of hypoxia affects progression and survival and with reliable hypoxia-imaging agents such as FMISO becoming available, treatments aimed at eradicating the hypoxic regions of malignant gliomas deserve further investigation. Methods are now available to allow coregistration of FMISO PET images with MRI images used with surgical navigational devices. Surgical resections could thereby target hypoxic regions and/or include implantation of therapeutic agents such as hypoxia-specific oncolytic viruses (46). Treatment plans with intensity-modulated radiation devices, for example, could be designed to target the hypoxic regions selectively with higher doses.

Hypoxia assessed with FMISO PET has been shown to be an important prognostic indicator in head and neck cancer (47). The question whether tirapazamine, TPZ, a hypoxia-activated

Table 3. Multivariate linear regression analyses of HV or T/B_{max} versus the MRI volumes, T0, T1Gd, and T2

Independent variables	Coefficient (SE)	P
HV		
T0	-1.23 (2.54)	0.64
T1Gd	2.45 (0.63)	0.002
T2	-0.21 (0.30)	0.49
R^2 = 0.77		
T/B $_{max}$		
T0	0.06 (0.09)	0.53
T1Gd	0.03 (0.02)	0.17
T2	-0.02 (0.01)	0.15
R^2 = 0.35		

Table 4. Multivariate analyses of survival or TTP versus HV, T1Gd volume, age, and KPS; or versus T/B_{max}, T1Gd volume, age, and KPS

Model covariates	Log hazard ratio coefficient (SE)	*P*
Survival		
HV	0.05 (0.02)	0.02
T1Gd	-0.048 (0.04)	0.18
Age	0.076 (0.04)	0.09
KPS	0.03 (0.03)	0.39
Log-partial likelihood = 11.7		
TTP		
HV	0.053 (0.022)	0.02
T1Gd	-0.064 (0.04)	0.09
Age	0.051 (0.041)	0.22
KPS	-0.0004 (0.03)	0.99
Log-partial likelihood = 11.9		
Survival		
T/B_{max}	1.57 (0.60)	0.01
T1Gd	0.01 (0.02)	0.58
Age	0.02 (0.05)	0.67
KPS	-0.09 (0.03)	0.78
Log-partial likelihood = 13.0		
TTP		
T/B_{max}	1.07 (0.53)	0.04
T1Gd	0.004 (0.02)	0.81
Age	0.003 (0.05)	0.96
KPS	-0.031 (0.031)	0.33
Log-partial likelihood = 8.9		

cytotoxin, improves the results of radiotherapy in this disease was investigated and reported by Rischin et al. (32). The patients with hypoxic tumors, as shown by FMISO PET, that received TPZ fared significantly better than the control patients with respect to the risk of locoregional failure. This outcome supported the efficacy of TPZ specifically in the presence of hypoxic disease. In gliomas, there has been no comparable study that segregated patients based on the presence of hypoxia as shown by FMISO PET. However, TPZ was ineffective at improving survival in a phase II study of 124 patients with glioblastoma multiforme (48). Based on the results of the head and neck study cited above, a newer hypoxia-selective cytotoxin, SN30000 (49), with better activity than TPZ may be worth examining in patients specifically preselected for the presence of hypoxia.

Many other chemotherapy approaches are coming to the fore. One is the hypoxia-activated anthraquinone AQ4N (banoxatrone), a prodrug that is selectively reduced in hypoxic tissues to AQ4, an inhibitor of topoisomerase II and a DNA intercalator (50). These actions sensitize tumors to chemotherapy and radiotherapy (51). Another promising agent is PR-104, a soluble phosphate ester that is converted *in vivo* to the corresponding alcohol PR-104A, which is activated in hypoxic conditions to a cytotoxic nitrogen mustard prodrug (52). Last, agents with the capacity to inhibit pathways leading to up-regulation of HIF1α are already available or on the horizon (50). When these agents are tested for efficacy against brain tumors, it will be important to assess whether they reduce the quantity and distribution of hypoxic disease, something that we and others have now shown to be feasible with FMISO PET.

Conclusion

Both greater volume of hypoxia (HV) and maximum intensity (T/B_{max}) in glioblastoma multiforme measured with FMISO PET before radiotherapy are strongly associated with poorer TTP and survival. HV and T/B_{max} showed statistically significant associations with TTP and survival in multivariate analyses that included age, KPS, and the TlGd MRI tumor volume. This type of imaging could be integrated into new regional and/or systemic treatment strategies to target hypoxia more aggressively in glioblastoma multiforme and could be applied to assess whether hypoxia-directed therapies actually achieve the goal of reducing the hypoxic burden of resistant disease.

Disclosure of Potential Conflicts of Interest

No potential conflicts of interest were disclosed.

References

1. Gray LH, Congor AD, Ebert M, Hornsey S, Scott OCA. The concentration of oxygen dissolved in tissues at the time of irradiation as a factor in radiotherapy. Br J Radiol 1953;26:638–48.
2. Hockel M, Vaupel P. Tumor hypoxia: definitions and current clinical, biologic, and molecular aspects. J Natl Cancer Inst 2001;93:266–76.
3. Liang BC. Effects of hypoxia on drug resistance phenotype and genotype in human glioma cell lines. J Neurooncol 1996;29:149–55.
4. Brizel DM, Sibley GS, Prosnitz LR, Scher RL, Dewhirst MW. Tumor hypoxia adversely affects the prognosis of carcinoma of the head and neck. Int J Radiat Oncol Biol Phys 1997;38:285–9.
5. Gatenby RA, Kessler HB, Rosenblum JS, et al. Oxygen distribution in squamous cell carcinoma metastases and its relationship to outcome of radiation therapy. Int J Radiat Oncol Biol Phys 1988; 14:831–8.
6. Kolstad P. Intercapillary distance, oxygen tension and local recurrence in cervix cancer. Scand J Clin Lab Invest 1968;106:145–57.
7. Brat DJ, Castellano-Sanchez AA, Hunter SB, et al. Pseudopalisades in glioblastoma are hypoxic, express extracellular matrix proteases, and are formed by an actively migrating cell population. Cancer Res 2004; 64:920–7.
8. Rampling R, Cruickshank G, Lewis AD, Fitzsimmons SA, Workman P. Direct measurement of *p*O2 distribution and bioreductive enzymes in human malignant brain tumors. Int J Radiat Oncol Biol Phys 1994;29: 427–31.
9. Evans SM, Judy KD, Dunphy I, et al. Comparative measurements of hypoxia in human brain tumors using needle electrodes and EF5 binding. Cancer Res 2004;64:1886–92.
10. Chapman JD, Engelhardt EL, Stobbe CC, Schneider RF, Hanks GE. Measuring hypoxia and predicting tumor radioresistance with nuclear medicine assays. Radiother Oncol 1998;46:229–37.
11. Rasey JS, Koh WJ, Grierson JR, Grunbaum Z, Krohn KA. Radiolabelled fluoromisonidazole as an imaging agent for tumor hypoxia. Int J Radiat Oncol Biol Phys 1989;17:985–91.
12. Rasey JS, Nelson NJ, Chin L, Evans ML, Grunbaum Z. Characteristics of the binding of labeled fluoromisonidazole in cells *in vitro*. Radiat Res 1990;122: 301–8.
13. Gross MW, Karbach U, Groebe K, Franko AJ, Mueller-Klieser W. Calibration of misonidazole labeling by simultaneous measurement of oxygen tension and labeling density in multicellular spheroids. Int J Cancer 1995;61:567–73.
14. Hall EJ. Radiobiology for the Radiologist. Philadelphia: Lippincott Williams and Wilkins; 2000.
15. Harris AL. Hypoxia—a key regulatory factor in tumour growth. Nat Rev Cancer 2002;2:38–47.
16. Denko NC, Fontana LA, Hudson KM, et al. Investigating hypoxic tumor physiology through gene expression patterns. Oncogene 2003;22:5907–14.
17. Said HM, Hagemann C, Staab A, et al. Expression patterns of the hypoxia-related genes osteopontin, CA9, erythropoietin, VEGF and HIF1α in human glioma *in vitro* and *in vivo*. Radiother Oncol 2007;83:398–405.
18. Stelzer KJ, Douglas JG, Mankoff DA, et al. Positron emission tomography-guided conformal fast neutron therapy for glioblastoma multiforme. Neuro-oncol 2008;10:88–92.
19. Macdonald DR, Cascino TL, Schold SCJ, Cairncross JG. Response criteria for phase II studies of supratentorial malignant glioma. J Clin Oncol 1990;8:1277–80.
20. Lewellen TK, Kohlmyer SG, Miyaoka RS, Schubert S, Stearns CW. Investigation of the count rate performance of General Electric Advance positron

emission tomograph. IEEE Trans Nucl Sci 1995; 42:1051–7.

21. Adamsen TC, Grierson JR, Krohn KA. A new synthesis of the labeling precursor for [^{18}F]-fluoromisonidazole. J Label Comp Radiopharm 2005;48:923–7.

22. Lim JL, Berridge MS. An efficient radiosynthesis of [^{18}F]fluoromisonidazole. Appl Radiat Isot 1993;44: 1085–91.

23. Grunbaum Z, Freauff SJ, Krohn KA, Wilbur DS, Magee S, Rasey JS. Synthesis and characterization of congeners of misonidazole for imaging hypoxia. J Nucl Med 1987;28:68–75.

24. Rajendran JG, Krohn KA. Imaging tumor hypoxia. In: Bailey DL, Townsend DW, Valk PE, Maisey MN, editors. Positron emission tomography, principles and practice. London: Springer-Verlag; 2002. p. 689–96.

25. Hsu SM, Raine L, Fanger H. Use of avidin-biotin-peroxidase complex (ABC) in immunoperoxidase techniques: a comparison between ABC and unlabeled antibody (PAP) procedures. J Histochem Cytochem 1981;29:577–80.

26. Harvey JM, Clark GM, Osborne CK, Allred DC. Estrogen receptor status by immunohistochemistry is superior to the ligand-binding assay for predicting response to adjuvant endocrine therapy in breast cancer. J Clin Oncol 1999;17:1474–81.

27. Mohsin SK, Weiss H, Havighurst T, et al. Progesterone receptor by immunohistochemistry and clinical outcome in breast cancer: a validation study. Mod Pathol 2004;17:1545–54.

28. Kalbfleisch JD, Prentice RL. The statistical analysis of failure time data. New York: Wiley; 1980.

29. Bruehlmeier M, Roelcke U, Schubiger PA, Ametamey SM. Assessment of hypoxia and perfusion in human brain tumors using PET with 18F-fluoromisonidazole and ^{15}O-H_2O. J Nucl Med 2004;45:1851–9.

30. Martin GV, Caldwell JH, Graham MM, et al. Noninvasive detection of hypoxic myocardium using fluorine-18-fluoromisonidazole and positron emission tomography. J Nucl Med 1992;33:2202–8.

31. Cher LM, Murone C, Lawrentschuk N, et al. Correlation of hypoxic cell fraction and angiogenesis with glucose metabolic rate in gliomas using ^{18}F-fluoromisonidazole, 18F-FDG PET, and immunohistochemical studies. J Nucl Med 2006;47:410–8.

32. Rischin D, Hicks RJ, Fisher R, et al. Prognostic significance of [^{18}F]-misonidazole positron emission tomography-detected tumor hypoxia in patients with advanced head and neck cancer randomly assigned to chemoradiation with or without tirapazamine: a substudy of Trans-Tasman Radiation Oncology Group Study 98.02. J Clin Oncol 2006; 24:2098–104.

33. Liu RS, Chu LS, Chu YK, Yen SH, Liao SQ, Yeh SH. Does β-oxidation occur in malignant neoplasm? A concurrent [C-11]acetate and [F-18]MISO study [abstract]. J Nucl Med 1999;40:239P.

34. Valk PE, Mathis CA, Prados MD, Gilbert JC, Budinger TF. Hypoxia in human gliomas: demonstration by PET with fluorine-18-fluoromisonidazole. J Nucl Med 1992;33:2133–7.

35. Evans SM, Jenkins WT, Shapiro M, Koch CJ. Evaluation of the concept of "hypoxic fraction" as a descriptor of tumor oxygenation status. Adv Exp Med Biol 1997;411:215–25.

36. Evans SM, Judy KD, Dunphy I, et al. Hypoxia is important in the biology and aggression of human glial brain tumors. Clin Cancer Res 2004;10:8177–84.

37. Grigsby PW, Malyapa RS, Higashikubo R, et al. Comparison of molecular markers of hypoxia and imaging with (60)Cu-ATSM in cancer of the uterine cervix. Mol Imaging Biol 2007;9:278–83.

38. Kaur B, Khwaja FW, Severson EA, Matheny SL, Brat DJ, Van Meir EG. Hypoxia and the hypoxia-inducible-factor pathway in glioma growth and angiogenesis. Neuro-oncol 2005;7:134–53.

39. Chan AS, Leung SY, Wong MP, et al. Expression of vascular endothelial growth factor and its receptors in the anaplastic progression of astrocytoma, oligodendroglioma, and ependymoma. Am J Surg Pathol 1998;22:816–26.

40. Varlet P, Guillamo JS, Nataf F, Koziak M, Beuvon F, Daumas-Duport C. Vascular endothelial growth factor expression in oligodendrogliomas: a correlative study with Sainte-Anne malignancy grade, growth fraction and patient survival. Neuropathol Appl Neurobiol 2000;26:379–89.

41. Allalunis-Turner MJ, Franko AJ, Parliament MB. Modulation of oxygen consumption rate and vascular endothelial growth factor mRNA expression in human malignant glioma cells by hypoxia. Br J Cancer 1999; 80:104–9.

42. Parliament MB, Allalunis-Turner MJ, Franko AJ, et al. Vascular endothelial growth factor expression is independent of hypoxia in human malignant glioma spheroids and tumours. Br J Cancer 2000;82: 635–41.

43. Zagzag D, Zhong H, Scalzitti JM, Laughner E, Simons JW, Semenza GL. Expression of hypoxia-inducible factor 1α in brain tumors: association with angiogenesis, invasion, and progression. Cancer 2000;88:2606–18.

44. Sondergaard KL, Hilton DA, Penney M, Ollerenshaw M, Demaine AG. Expression of hypoxia-inducible factor 1α in tumours of patients with glioblastoma. Neuropathol Appl Neurobiol 2002;28:210–17.

45. Jensen RL. Hypoxia in the tumorigenesis of gliomas and as a potential target for therapeutic measures. Neurosurg Focus 2006;20:1–12.

46. Post DE, Devi NS, Li Z, et al. Cancer therapy with a replicating oncolytic adenovirus targeting the hypoxic microenvironment of tumors. Clin Cancer Res 2004; 10:8603–12.

47. Rajendran JG, Schwartz DL, O'Sullivan J, et al. Tumor hypoxia imaging with [F-18] fluoromisonidazole positron emission tomography in head and neck cancer. Clin Cancer Res 2006;12:5435–41.

48. Del Rowe J, Scott C, Werner-Wasik M, et al. Single-arm, open-label phase II study of intravenously administered tirapazamine and radiation therapy for glioblastoma multiforme. J Clin Oncol 2000;18: 1254–9.

49. Hay MP, Hicks KO, Siim BG, et al. Tricyclic triazine 1,4-dioxides: a new class of hypoxia-selective cytotoxins with improved extravascular transport compared to tirapazamine. Eur J Cancer Suppl 2006;4: 82–3.

50. Rosenberg A, Knox S. Radiation sensitization with redox modulators: a promising approach. Int J Radiat Oncol Biol Phys 2006;64:343–54.

51. Atkinson SJ, Loadman PM, Sutton C, Patterson LH, Clench MR. Examination of the distribution of the bioreductive drug AQ4N and its active metabolite AQ4 in solid tumours by imaging matrix-assisted laser desorption/ionisation mass spectrometry. Rapid Commun Mass Spectrom 2007;21:1271–6.

52. Dorie MJ, Ahn G-O, Menke D, et al. Prediction of antitumor activity of PR-104, a new hypoxia activated mustard, using measurements of DNA interstrand crosslinks by the comet assay. Proc Am Assoc Cancer Res 2006;47:1334–5.